Inorganic Chemistry

ARTICLE

pubs.acs.org/IC

New Ternary and Quaternary Barium Nitride Halides; Synthesis and Crystal Chemistry

Andrew S. Bailey,[†,⊥] Robert W. Hughes,[‡] Peter Hubberstey,[†] Clemens Ritter,[§] Ronald I. Smith,[∥] and Duncan H. Gregory*[,‡]

[†]School of Chemistry, University of Nottingham, Nottingham NG7 2RD, United Kingdom

[‡]WestCHEM, School of Chemistry, University of Glasgow, Glasgow G12 8QQ, United Kingdom

[§]Institut Laue-Langevin, 6, rue Jules Horowitz, BP 156−38042, Grenoble, Cedex 9, France

[∥]ISIS Pulsed Neutron and Muon Source, Science and Technology Facilities Council, Rutherford Appleton Laboratory, Didcot, OX11 0QX, United Kingdom

Supporting Information

ABSTRACT: New ternary and quaternary nitride halides, $Ba_2N(X,X')$ (X = F, Cl, Br; X′ = Br, I), have been synthesized from the high temperature reactions of barium subnitride with the respective barium halides under an inert atmosphere. The former include the first fully characterized barium nitride halides for X other than F, and the latter are the first examples of barium nitride mixed halides. The variation in structure with composition has been investigated by powder X-ray and powder neutron diffraction techniques. The heavier ternary and quaternary nitride halides (X, X′ = Cl, Br, I) crystallize in the hexagonal space group $R\bar{3}m$, with the *anti*-α-$NaFeO_2$ structure. Ba_2NF forms with both an *anti*-α-$NaFeO_2$ structure, in which N^{3-} and F^- are ordered and an anion-disordered simple rock salt structure. The hexagonal polymorph of Ba_2NF is the only example to date of a nitride fluoride adopting this layered structure. Both the ternary and the quaternary compounds display very weak, temperature independent paramagnetism.

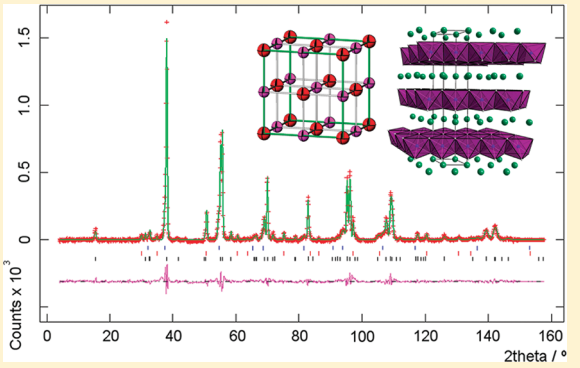

INTRODUCTION

The field of inorganic nitride chemistry has shown considerable growth over the past two decades.[1−3] It is perhaps unexpected that some of the more unusual and interesting nitrides are formed by the alkali and alkaline earth metals.[4,5] The group 2 metals (A) form nitrides with A−N bonding and structures that change dramatically as one descends the group; the lighter metals (Be to Ca) form ionic, insulating or semiconducting, salt-like compounds[6−8] whereas the heavier members of the group (Ca to Ba) form subnitrides with low-dimensional structures and metallic properties.[9−11]

One of the simplest families of compounds produced experimentally from the nitrides are the nitride halides A_2NX (X = F−I), and indeed some members have been known for decades.[12−17] More recently the structures of some of these nitride halide materials have been examined in detail through single-crystal diffraction techniques.[18−23] Recent work has suggested that the ternary nitride halide phase systems are more complex than originally envisaged and that the structures and anion distributions are sensitive to both the halide (X) and the conditions of synthesis.[20,21] The types of structure seen in the nitride halides vary from simple rock salt analogues (for example, Sr_2NF)[17] to layered materials (for example, Ca_2NCl).[18] Indeed in some systems, different structural polymorphs have been demonstrated to exist, for example, Ca_2NF has been reported variously to form with a simple cubic rock salt,[17] a doubled cubic rock salt,[23] or an ordered rock salt-derived tetragonal cell.[20] Moreover, variation in structure, stoichiometry, and anion distribution is likely to have profound effects on electronic properties. For example, in the Mg−N−F system, one moves from insulating MgF_2 (calculated direct band gap, E_g, of 6.8 eV) through Mg_3NF_3 (E_g = 3.6 eV) and L−Mg_2NF (E_g = 2.1 eV) to semiconducting Mg_3N_2 with a calculated direct band gap of 1.6 eV (2.8 eV experimentally).[24]

In comparison to the other group 2 metals, nitride halides of barium are rather less explored. Ehrlich et al. suggested the existence of the compositions Ba_2NCl, Ba_2NBr, and Ba_6NI_9 from the reaction of "Ba_3N_2" with BaX_2.[13] PXD produced patterns that could not be matched to the starting materials, but no structures were published. A simple rock salt structure for Ba_2NF had been described by Ehrlich et al.[17] which has recently been supported by a subambient temperature single crystal structure determination by Seibel and Wagner.[22]

Received: June 12, 2011
Published: August 26, 2011

Table 1. $Ba_2N(XX')$ Samples Synthesized

sample no.	reactants; ratio	nominal stoichiometry
1	Ba_2N: BaF_2; 2:1	Ba_2NF
2	Ba_2N: $BaCl_2$; 2:1	Ba_2NCl
3	Ba_2N: $BaCl_2$: $BaBr_2$; 10:4:1	$Ba_2NCl_{0.8}Br_{0.2}$
4	Ba_2N: $BaCl_2$: $BaBr_2$; 10:3:2	$Ba_2NCl_{0.6}Br_{0.4}$
5	Ba_2N: $BaCl_2$: $BaBr_2$; 10:2:3	$Ba_2NCl_{0.4}Br_{0.6}$
6	Ba_2N: $BaCl_2$: $BaBr_2$; 10:1:4	$Ba_2NCl_{0.2}Br_{0.8}$
7	Ba_2N: $BaBr_2$; 2:1	Ba_2NBr
8	Ba_2N: $BaBr_2$: BaI_2; 10:4:1	$Ba_2NBr_{0.8}I_{0.2}$

In our previous studies we examined the synthesis of ternary, quaternary, and quintinary alkaline earth nitride halides of calcium and strontium, and the effect that varying the halide has on the structure.[25−28] In this work we have probed the existence, structure, and stoichiometry of compounds in the barium−nitrogen−halogen systems and have successfully synthesized a tranche of new compounds containing halides varying from F^- through Cl^- and Br^- to I^-. Powder X-ray and neutron diffraction measurements have enabled us to determine definitive structural models for a new hexagonal polymorph of Ba_2NF, the ternary compounds Ba_2NCl and Ba_2NBr, and a series of new quaternary mixed halides, $Ba_2NX_{(1-y)}X'_y$ (X = Cl, Br, I).

EXPERIMENTAL SECTION

Caution! Ba_2N and all derived nitride halide materials are extremely air and moisture sensitive. Handling must be carried out in an argon atmosphere, which presents difficulties in characterization. Even with the use of a dedicated airtight powder X-ray diffraction (PXD) sample holder,[29] some sample hydrolysis was observed over longer scans.

Synthesis of Ba_2N. Ba_2N was prepared by reaction of barium with nitrogen using liquid sodium as a solvent medium. All manipulations were carried out in an inert atmosphere. In an argon filled glovebox a piece of barium (approximately 15 g, Alfa, 99+ %) was cut from a larger ingot, and the covering oxide layer was removed with a file. The clean metal was submerged in molten sodium (Riedel-de Haën, >99%) contained within a stainless steel crucible. The crucible was then sealed inside a stainless steel reaction vessel fitted with a coldfinger and a gas-line connection and removed from the glovebox. The vessel was evacuated and filled with nitrogen gas before being heated for 48 h at 973 K. Upon cooling the vessel was placed under a vacuum of 10^{-4} Torr and heated for 24 h at 723 K to remove the sodium. Once cooled to room temperature the vessel was opened in an argon filled glovebox. The product was a black crystalline solid deposited within and around the stainless steel crucible. The product was ground to give a fine dark brown powder, and PXD was used to confirm phase purity by comparison to ICDD card 79-4939.

Synthesis of Ba_2NX (X = F, Cl, Br). All manipulations were carried out in an argon-filled glovebox unless stated otherwise. Ternary barium nitride halides were prepared by the reaction of barium nitride, Ba_2N, with the relevant barium halide, BaX_2 (X = F, Cl, Br):

$$2Ba_2N + BaX_2 \rightarrow 2Ba_2NX + Ba \quad (1)$$

The barium halides (X = F (Aldrich, 99.9%), Cl (Aldrich, 99.9%), Br (Strem, 99%), I (Alfa, 99%)) were dried prior to use. Each was heated under a dynamic vacuum (10^{-4} atm) for 24 h at 423 K.

Powders of Ba_2N and BaX_2 were intimately mixed and pelletized. The pellets were wrapped in a molybdenum foil liner before being welded inside a stainless steel crucible. The crucible was then fired for 5 days at 998 K under an argon atmosphere (to prevent crucible oxidation), before being slow cooled at 20 Kh^{-1}. The crucibles were then opened in a nitrogen filled glovebox with pipe cutters.

Synthesis of $Ba_2NX_{1-y}X'_y$ (X,X' = Cl, Br, I; 0 < y < 1). All manipulations were carried out in an argon-filled glovebox unless stated otherwise. Quaternary barium nitride mixed halides were prepared according to the following scheme:

$$2Ba_2N + (1-y)BaX_2 + yBaX'_2 \rightarrow 2Ba_2NX_{1-y}X'_y + Ba \quad (2)$$

Samples were synthesized following a similar procedure to that employed for the ternary compounds above with pelletized powders sealed in Mo foil lined steel crucibles. All compounds were fired for 5 days at 998 K and slow cooled at 20 Kh^{-1}. All crucibles were opened in a nitrogen filled glovebox. The reagents, starting ratios and target products (**1**−**8**) are summarized in Table 1.

Powder X-ray Diffraction. The barium subnitride starting material, ternary and quaternary products were initially characterized by powder X-ray diffraction (PXD). Data were collected using a Philips X-pert diffractometer operating with copper K_α radiation. Scans were carried out in Bragg−Brentano geometry from 5−80° in 2θ with a step size of 0.02° over 50 min. Additionally for **7** and **8**, further scans were carried out from 5−120° in 2θ with a step size of 0.02° over 14 h to provide data suitable for Rietveld refinement. Because of the air-sensitive nature of the products, a dedicated airtight aluminum sample holder with Mylar windows was employed.[29] Data were analyzed by Philips Automated Powder Diffraction software. Phase identification was carried out using Philips PC-IDENTIFY to access the ICDD PDF database. Unit cells were indexed and lattice parameters refined using DICVOL91.[30]

Powder Neutron Diffraction. Constant wavelength (CW) powder neutron diffraction (PND) data for Ba_2NF (**1**) were collected on the D1A instrument at the Institut Laue-Langevin, Grenoble, France. A sample of approximately 2 g was sealed inside a 10 mm diameter vanadium sample can using a gold seal. A germanium monochromator was used to select an incident wavelength of 1.909 Å.

Time of flight (ToF) PND data for Ba_2NCl (**2**) and $Ba_2NCl_{1-y}Br_y$ (y = 0.2, 0.4, 0.6, 0.8) (**3**−**6**) were collected using the medium resolution, high intensity POLARIS diffractometer at the ISIS facility, Rutherford Appleton Laboratory, U.K. For each sample, 1−3 g of material was sealed in an electron beam welded vanadium can, made airtight using an indium wire gasket. All diffraction experiments were performed at 298 K with collection times of 1−2 h per sample. Diffraction data were collected using the ^{3}He tube low angle and backscattering detector banks at $\langle 2\theta \rangle$ = 35° and $\langle 2\theta \rangle$ = 145° and the ZnS scintillator detector bank at $\langle 2\theta \rangle$ = 90°.

Rietveld Refinement. Rietveld refinement against all types of diffraction data was performed using the General Structure Analysis System (GSAS) via the windows-based EXPGUI interface.[31,32] The major phase in each sample (**1**−**8**) was fitted using the *anti*-α-$NaFeO_2$ structure as an initial starting model. Lattice parameters obtained from indexing PXD data were used for the initial values in the refinement.

Refinements followed a similar strategy for **1**−**8**, although the background and peak shape functions selected were instrument-dependent. For **1** collected on D1A, the first parameters refined were the background coefficients (GSAS Function 1, a Chebyschev polynomial) and scale factor; this was followed by refinement of the unit cell parameters. The atomic parameters, peak profile parameters, and isotropic temperature factors were varied subsequently. Modeling of the peak shapes was carried out using CW function 2, the Thompson−Cox−Hastings pseudo-Voigt function. Additional phases were added once refinement of the main phases was almost complete, and refined using the same approach. The anisotropic temperature factors of the main phase were one of the last variables to be refined, while in the final refinement cycles all parameters were simultaneously varied.

The POLARIS ToF PND data taken from the three detector banks at low angle $\langle 2\theta \rangle$ = 35°, $\langle 2\theta \rangle$ = 90° and backscattering angles at $\langle 2\theta \rangle$ = 145°

dx.doi.org/10.1021/ic201264u |*Inorg. Chem.* 2011, 50, 9545–9553

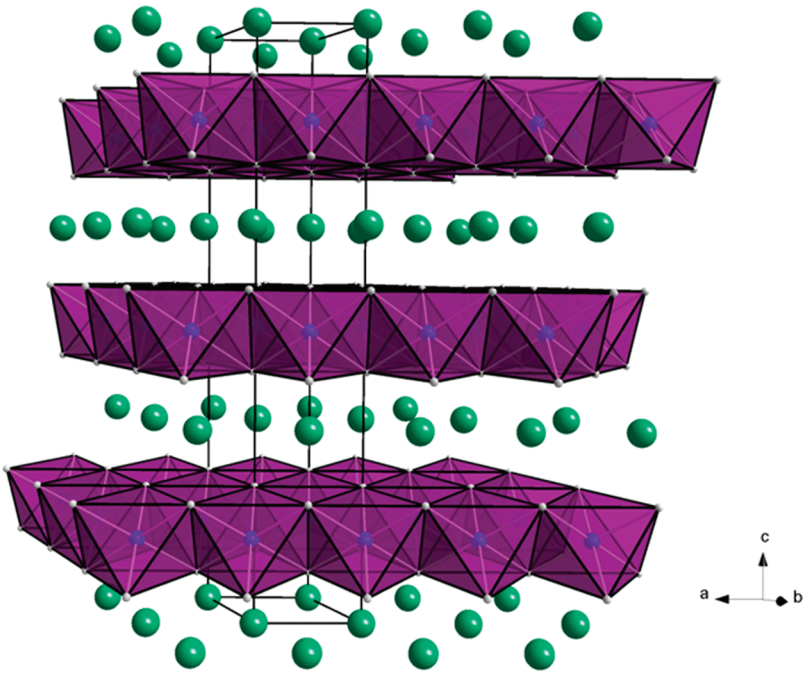

Figure 1. Structural representation of the A_2NX structure (*anti*-α-$NaFeO_2$ type). The $[A_2N]^+$ layers are composed of edge sharing NA_6 octahedra. Halide ions, X^-, reside between the positively charged layers.

were used in the refinements of **2**− **6**. The background was fitted using the exponential expansion function (Function 4 in GSAS), and the peak shape was modeled with ToF Function 3, a convolution of back-to-back exponentials with a pseudo-Voigt function with Lorentzian broadening.

For **7** and **8** the refinements were carried out against PXD data. The background was modeled with GSAS Function 1, a Chebyschev polynomial, and the peakshape with the Thompson−Cox−Hastings pseudo-Voigt function (Function 2). A March Dollase function was used to model (00*l*) preferred orientation arising from the flat plate experiments.

Magnetic Measurements. Variable temperature magnetic susceptibility measurements were performed for **1**−**8** (ca. 10−25 mg for each sample) using a Quantum Design MPMS-XL 5T SQUID magnetometer. All samples were loaded in a nitrogen-filled, recirculating glovebox. Data were collected between 5−300 K under fields of 1000 Oe with points at 1 K intervals from 5−30 and 5 K intervals between 30−300 K. Data were corrected for core diamagnetism and the diamagnetic contribution of the sample holders (gelatin capsules).

RESULTS AND DISCUSSION

Ba_2N Starting Material. After distillation of the sodium from the reaction, the Ba_2N product was left as a brown/black solid which became a dark brown fine powder upon grinding. PXD data confirmed a pure phase product by comparison to the ICDD database. (PXD data can be found in the Supporting Information, Figure SI1). The cell parameters were refined to a = 4.1146(3) Å and c = 22.603(2) Å. This is slightly larger in a than previously reported (a = 3.99−4.05 Å) although the c parameter falls within previously reported limits (c = 22.08−22.70 Å).[33−38]

Ba_2NF. Reactions consistently led to powdered black/gray products. During attempts to synthesize powder samples of Ba_2NF, PXD revealed that two phases were present in addition to a BaF_2 impurity phase. Some of the outstanding reflections could be indexed to cubic Ba_2NF (space group $Fm\bar{3}m$),[22] but patterns also contained a significant number of additional higher intensity peaks. It was possible to index these reflections to a hexagonal cell (a = 4.00(5), c = 19.7(2) Å) in space group $R\bar{3}m$, which is consistent with the *anti*-α-$NaFeO_2$ structure adopted by other alkaline earth nitride halides A_2NX (A= Ca, Sr. X = Cl, Br).[26,27] This structure is a filled *anti*-$CdCl_2$-type formed from $[NBa_2]^+$ slabs and halide ions, F^-, which reside in the octahedral voids between the positively charged layers. This thus creates alternating edge sharing layers of NBa_6 and FBa_6 octahedra in a cubic close packed arrangement. A representation of this structure can be seen in Figure 1, and the structure is discussed in more detail elsewhere.[26,27] This is the first incidence of a nitride fluoride crystallizing with this structure. Previous studies of A_2NF (A = Mg−Ba) have revealed compounds which adopt cubic (simple or ordered) rock salt structures or tetragonal (ordered, rock salt-derived) structures only.[16,17,20−23]

Given the mixture of light and heavy atoms in the structure and the similarity of form factor for isoelectronic N^{3-} and F^-, obtaining a complete structure solution for **1** from PXD data alone was not trivial. PND data were collected to address this problem since there is sufficient contrast in the coherent neutron scattering lengths to obtain a complete description of the structure (Ba b = 5.07 fm; N b = 9.36 fm, F b = 5.65 fm).[39] The refinement was performed employing the *anti*-α-$NaFeO_2$ structure, as adopted by $Ca(Sr)_2NCl(Br)$ compounds, to model the majority phase, utilizing the cell parameters from the indexed PXD data. The refinement progressed smoothly and converged to produce a good fit to the data. Attempts to refine occupancies of the anion sites to investigate possible N/F disorder reduced the quality of the fit, increased R-factors, and caused some parameters to become unstable. The evidence suggests, therefore, that an ordered model is appropriate as has been seen for other layered A_2NX compounds.[26,27]

As alluded to above, the fit was improved by the addition of two secondary phases; the first was a cubic Ba_2NF phase following the single crystal model of Seibel and Wagner,[22] while the second was BaF_2. The quality of the diffraction data allowed

dx.doi.org/10.1021/ic201264u |*Inorg. Chem.* 2011, 50, 9545–9553

Table 2. Refined Crystallographic Parameters for Ba_2NF (1, 1′) from CW PND data at 298 K

		Ba_2NF (1)		Ba_2NF (1′)	
diffraction experiment, instrument		CW PND, D1A		CW PND, D1A	
crystal system		hexagonal		cubic	
space group		$R\bar{3}m$ (No. 166)		$Fm\bar{3}m$ (No. 225)	
a/Å		4.0242 (2)		5.7945 (6)	
c/Å		19.975 (1)			
V/Å^3		280.14 (2)		194.56 (7)	
Z		3		1	
M/g mol^{-1}		307.659		307.659	
calculated density, ρ_x/g cm^{-3}		5.471		5.252	
z (Ba) (6c; 0,0,z)		0.2453(4)			
$U_e \times 100$/Å^{2a}	Ba	6c (0,0,z)	1.78[b]	4a (0,0,0)	1.12 (3)
	N	3a (0,0,1/2)	2.40[b]	4b (1/2,1/2,1/2)[c]	2.54 (2)
	F	3b (0,0,0)	4.43[b]	4b (1/2,1/2,1/2)[c]	2.54 (2)
phase fraction		76.7(1)%		16.4(1)%	
no. of data		1459			
no. of parameters		18			
R_{wp}		0.0460			
R_p		0.0340			
reduced χ^2		5.397			

[a] U_e, the equivalent thermal displacement factor, is defined as one-third of the sum of the diagonal elements of the orthogonalized U_{ij} tensor $U_{ij} = \exp[-2\pi^2(U_{11}h^2a^{*2} + U_{22}k^2b^{*2} + U_{33}l^2c^{*2} + 2U_{12}hka^*b^* + 2U_{23}klb^*c^* + 2U_{13}hla^*c^*)]$. [b] Displacement factors refined anisotropically. [c] Site occupied statistically by 50% N and 50% F.

us to obtain an accurate structural model for the secondary nitride fluoride phase (in addition to the Ba_2NF major phase). The anion distribution in the minority Ba_2NF phase was confirmed as a disordered one with N and F statistically occupying the 4b (1/2,1/2,1/2) site. The results of the refinement can be found in Table 2. Anisotropic thermal displacement parameters are detailed in the Supporting Information. The fit to the data is shown in the profile plot in Figure 2.

The refined *anti*-α-$NaFeO_2$ structure of the majority phase Ba_2NF has a c parameter that is notably shorter than related compounds. The unfilled subnitride Ba_2N[33] has a c parameter of 22.425(4) Å, decreasing to 20.493(4) Å in the hydride Ba_2NH[40] and 19.975(1) Å in the fluoride reported here. This is due to the repulsion between the $[Ba_2N]^+$ layers being reduced relative to Ba_2N by the inclusion of increasingly electronegative anions (vs size effects). Our CW PND refinement demonstrated that our sample contained approximately 16% by weight of cubic Ba_2NF (**1′**). The refined cubic a parameter of the rock salt phase is larger than that reported by Seibel and Wagner (5.6796(19) Å) but it should be noted that our PND data were collected at 298 K, while the previously reported single crystal X-ray data were collected at 100 K.[22] Ehrlich et al. had earlier reported a cubic phase of Ba_2NF with a lattice parameter of 5.69 Å but there is no record of the temperature at which their data were collected.[17] Ba_2NF might be regarded loosely as a "pseudo-oxide" (given that the nitride fluoride and oxide are isoelectronic) and the cubic phase is isostructural, of course with BaO. In this respect, it is noteworthy that the cubic lattice parameter in the nitride fluoride is larger than that of barium oxide (5.517 Å)[41] (and hence the Ba−(N,F) bond longer than the equivalent Ba−O distance).

Table 3 gives a comparison of important bond lengths between the hexagonal and cubic polytypes of Ba_2NF and the previously reported data for the cubic variant. The Ba−Ba distances in the

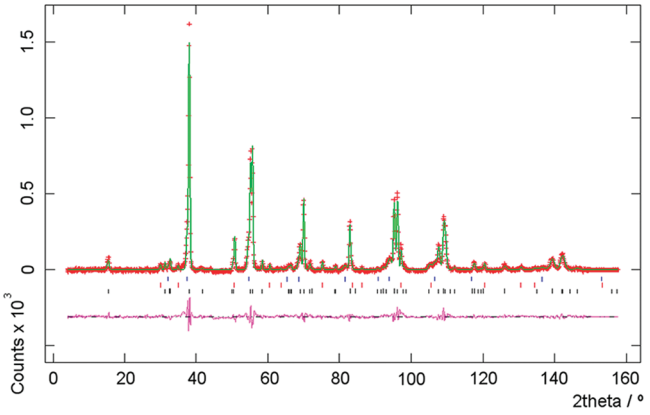

Figure 2. Rietveld refinement profile for Ba_2NF from CW PND data. Crosses indicate the observed data, the upper continuous line shows the calculated profile and the lower continuous line the difference profile. Tick marks show reflection positions for hexagonal Ba_2NF (lower), BaF_2 (middle), and cubic Ba_2NF (upper).

cubic structure reported here (4.097(1) Å) are greater than those in the hexagonal phase (4.024(1) Å), by about 2%. The Ba−Ba distance in the literature structure is marginally reduced because of the lower data collection temperature.[22] The cubic rock salt phase has one anion site occupied statistically by N^{3-} and F^- and the Ba−(N,F) distance (2.8973(4) Å) in the cubic phase is close to the mean of the Ba−F and Ba−N values (2.859 (1) Å) in the hexagonal polytype. Interestingly and given also the unusually low coordination number of 6 for Ba in Ba_2NX compounds, the Ba−F distances in the hexagonal Ba_2NF polytype (**1**) are significantly longer than the bond lengths in either ambient or high pressure forms of BaF_2 (2.6831 (2) Å and 2.663 (1) Å (at 1.5 GPa) respectively).[42,43] There is also an increase in the Ba−N distances compared to those

dx.doi.org/10.1021/ic201264u |*Inorg. Chem.* 2011, 50, 9545–9553

Table 3. Selected Interatomic Distances and Angles in Hexagonal and Cubic Ba_2NF (1, 1′) from CW PND Data at 298 K

	Ba_2NF (1)	Ba_2NF (1′)	Ba_2NF[22a]
crystal system, space group	hexagonal, $R\bar{3}m$ (No. 166)	cubic, $Fm\bar{3}m$ (No. 225)	cubic, $Fm\bar{3}m$ (No. 225)
Ba−Ba/Å	3.9100(1) × 3		
Ba−Ba/Å	4.0242(2) × 6	4.0974(4) × 12	4.016 (4) × 12
Ba−N/Å	2.8055(1) × 3	2.8973(4) × 6	2.840 (2) × 6
Ba−X/Å	2.9128(1) × 3	2.8973(4) × 6	2.840 (2) × 6
Ba−N−Ba/deg	91.649 (2)	90.0 × 6	90.0 × 6
Ba−X−Ba/deg	87.386 (3)	90.0 × 6	90.0 × 6

[a] Data collected at 100 K.

Table 4. Refined Crystallographic Parameters for $Ba_2NCl_{(1-y)}Br_y$ (2−6) from ToF PND Data at 298 K

		Ba_2NCl (2)	$Ba_2NCl_{0.8}Br_{0.2}$ (3)	$Ba_2NCl_{0.6}Br_{0.4}$ (4)	$Ba_2NCl_{0.4}Br_{0.6}$ (5)	$Ba_2NCl_{0.2}Br_{0.8}$ (6)
diffraction experiment, instrument				TOF PND, POLARIS		
crystal system				hexagonal		
space group				$R\bar{3}m$ (No. 166)		
a/Å		4.1023 (1)	4.1202 (1)	4.1212 (1)	4.1348 (1)	4.1388 (1)
c/Å		22.6679 (2)	22.7619 (5)	22.9580 (4)	23.1668 (4)	23.3045 (4)
V/Å^3		329.487 (3)	334.644 (10)	337.681(7)	343.017 (7)	345.717 (7)
Z		3	3	3	3	3
M/g mol^{-1}		324.113	333.004	341.894	350.784	359.674
calculated density, ρ_x/g cm^{-3}		4.900	4.956	5.074	5.104	5.197
z (Ba) (6c; 0,0,z)		0.7682 (1)	0.7686 (1)	0.7695 (1)	0.7701 (1)	0.7705 (1)
U_e × 100/Å^{2a,b}	Ba (6c)	0.73 (1)	1.13 (2)	1.10 (3)	0.95 (2)	1.08 (2)
	N (3a)	1.63 (2)	2.23 (3)	2.12 (3)	1.95 (2)	2.14 (2)
	X (3b)	1.75 (2)	1.67 (3)	1.75 (4)	1.68 (3)	1.77 (3)
Cl: Br		1:0	0.801: 0.199 (7)	0.554: 0.446 (8)	0.386: 0.614 (5)	0.178: 0.822 (6)
no. of data		13696	13035	13481	13481	13692
no. of parameters		25	30	27	30	30
R_{wp}		0.0176	0.0230	0.0273	0.0230	0.0295
R_p		0.0392	0.0434	0.0574	0.0508	0.0485
reduced χ^2		1.543	2.987	3.307	2.047	5.474

[a] U_e, the equivalent thermal displacement factor, is defined as one-third of the sum of the diagonal elements of the orthogonalized U_{ij} tensor $U_{ij} = \exp[-2\pi^2(U_{11}h^2a^{*2} + U_{22}k^2b^{*2} + U_{33}l^2c^{*2} + 2U_{12}hka^*b^* + 2U_{23}klb^*c^* + 2U_{13}hla^*c^*)]$. [b] Displacement factors refined anisotropically.

in the unfilled subnitride, Ba_2N (in which Ba is three-coordinate to nitrogen).[33] It was our intention to probe the structure by CW PND at variable temperature to explore the phase change behavior on heating and cooling. Unfortunately the Ba_2NF material is highly reactive at elevated temperature and reacted vigorously with the vanadium sample can during our variable temperature neutron experiment, compromising the sample environment and preventing elucidation of any phase change behavior at this time.

The range of A_2NF materials in the literature form a variety of structures, although mainly rock salt or rock salt-related in nature. In simple rock salt structures, the N^{3-} and F^- anions must be disordered to maintain the simple cubic cell. Ordering of the anions leads to structures with larger cells, such as the tetragonal cell formed by L-Mg_2NF[16] and Ca_2NF,[20] or the cubic cell, doubled along all axes, exhibited by Sr_2NF[21] and Ca_2NF.[23] Compositional variation may also lead to ordered structures such as the rock salt related cubic cell of Mg_3NF_3 where 1/4 of the magnesium sites are empty in an ordered fashion.[16] The synthesis regime almost certainly plays a role in determining the structure formed. Heat and pressure (1100 °C, 25 kbar) transform the tetragonal, ordered L−Mg_2NF into the disordered cubic H−Mg_2NF.[16] By analogy in oxide rock salt materials, *cation* disorder is seen to increase with heating. For example, in oxide series such as $Li_2(Ti_{1-x}Zr_x)O_3$ it is possible to quench the disordered structures from high temperature for compounds of certain values of x.[44] In nitride fluoride systems, ordered structures are typically seen in single crystal samples which have been cooled slowly from the melt, favoring ordering of the anions.[20,21,23] By contrast, simple rock salt phases were originally reported for powders prepared by solid state methods, although magnesium ordered structures exist synthesized as powders and single crystals of rock salt structured Ba_2NF exhibit anion disorder.[22] The Ba_2NF phase we have reported here (**1**; hexagonal α-$NaFeO_2$ structure) is another example of an ordered structure formed on slow cooling. Uniquely among alkaline earth nitride fluorides to date, hexagonal Ba_2NF is also a phase in competition with a disordered cubic rock salt (**1′**). Later below, we consider the possible effects of cation and anion composition on structural stability in group 2 metal nitride halides, but systematic probing of the phase space at and away from thermal equilibrium would clarify the relationships between the different ordered and disordered phases observed for A_2NF materials.

dx.doi.org/10.1021/ic201264u |*Inorg. Chem.* 2011, 50, 9545–9553

Table 5. Selected Interatomic Distances and Angles for $Ba_2NCl_{(1-y)}Br_y$ (2−6) from ToF PND Data at 298 K

	2	3	4	5	6
crystal system space group			hexagonal, $R\bar{3}m$ (No. 166)		
3 × Ba−Ba/Å	3.77962 (2)	3.79477 (4)	3.77639 (4)	3.77708 (3)	3.78009 (4)
6 × Ba−Ba/Å	4.10225 (2)	4.12023 (3)	4.12118 (4)	4.13484 (3)	4.13881 (4)
3 × Ba−N/Å	2.78900 (1)	2.80074 (2)	2.79487 (2)	2.80015 (2)	2.80262 (2)
3 × Ba−X/Å	3.29808 (2)	3.31958 (3)	3.35131 (3)	3.38344 (2)	3.40062 (3)
Ba−N−Ba/deg	94.688 (1)	94.709 (1)	95.011 (1)	95.178 (1)	95.187 (1)

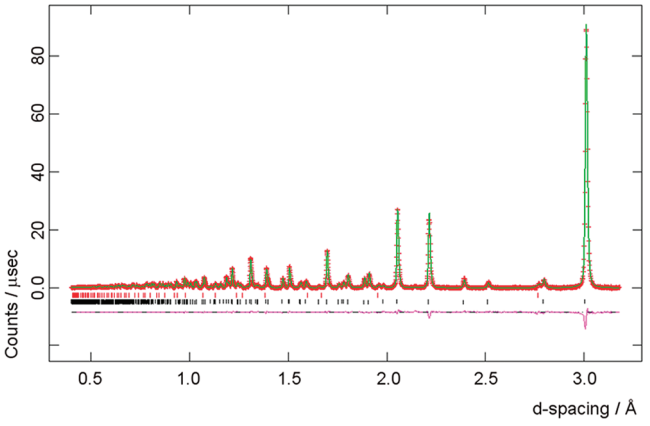

Figure 3. Rietveld refinement profile for Ba_2NCl from ToF PND data ($\langle 2\theta \rangle$ = 145° detector bank). Crosses indicate the observed data, the upper continuous line shows the calculated profile, and the lower continuous line the difference profile. Tick marks show reflection positions for Ba_2NCl (lower) and BaO (upper).

$Ba_2N(X,X')$ (X, X′ = Cl, Br, I). The series $Ba_2NCl_{(1-y)}Br_y$ (**2**−**6**) produced powdered products that were varying shades of purple reaching a brown coloration by y = 1, and all appeared from initial inspection of the PXD data to be single phase *anti*-α-$NaFeO_2$-type structures. Indexing the data showed an increase in both *a* and *c* parameters with increasing y commensurate with the progressive introduction of the larger halide anion into the system (ionic radii of 1.82 Å for Br^- vs 1.67 Å for Cl^-).[45] Initial short scans of the ternary nitride bromide, Ba_2NBr (**7**) and the brown quaternary bromide iodide, $Ba_2NBr_{0.8}I_{0.2}$ (**8**), showed reflections corresponding to *anti*-α-$NaFeO_2$ type structures to be present, and data indicated that both samples were single phase by PXD. It is notable, however, that when reactions with higher ratios of $BaI_2/BaBr_2$ were attempted (i.e., y > 0.2 in eq 2), the diffraction data became progressively poorer and additional unidentified reflections grew in intensity with increasing y. The origin of these reflections is under current investigation. By y = 1 there were no peaks that could be assigned to an *anti*-α-$NaFeO_2$ type structure. No convincing match was made when comparing reflections to a pattern of the Ba_6NI_9 phase proposed by Ehrlich et al.[13] Magnetometry measurements revealed that each of the samples **1**−**8** exhibited very weak temperature independent paramagnetic behavior (typically $\chi_M \sim 5 \times 10^{-6}$ emu mol^{-1}) suggestive of intrinsically diamagnetic materials with low levels of alkaline earth metal impurities (as corroborated by Rietveld refinement data) and consistent with other alkaline earth nitride halides.[26−28]

ToF PND data were collected for **2**−**6** and refinements performed using *anti*-α-$NaFeO_2$ type A_2NX structures as starting models. All refinements progressed smoothly to convergence.

Table 6. Refined Crystallographic Parameters for $Ba_2NBr_yI_{(1-y)}$ from PXD Data at 298 K

		Ba_2NBr (7)	$Ba_2NBr_{0.8}I_{0.2}$ (8)
diffraction experiment, instrument		CW XRD, Xpert	CW XRD, Xpert
crystal system		hexagonal	hexagonal
space group		$R\bar{3}m$ (No. 166)	$R\bar{3}m$ (No. 166)
a/Å		4.1534 (1)	4.1578 (2)
c/Å		23.348 (1)	23.538 (1)
V/Å^3		352.50 (12)	357.74 (3)
Z		3	3
M/g mol^{-1}		368.565	377.965
calculated density, ρ_x/g cm^{-3}		5.291	5.256
z (6*c*; 0,0,*z*)		0.7698 (4)	0.7710 (1)
U_{iso} × 100/Å^2	Ba (6*c*)	3.09 (2)	3.63 (2)
	N (3*a*)	5.42 (2)	8.27 (1)
	X (3*b*)	3.81 (4)	3.35 (3)
Br: I		1: 0	0.812: 0.188 (9)
no. of data		5750	5750
no. of parameters		14	23
R_{wp}		0.1497	0.1347
R_p		0.1153	0.1022
reduced χ^2		1.526	1.667

The inclusion of minor impurity phases improved the fits significantly, and many of these phases are not unexpected given that barium is expected to be generated in the reactions from eq 3 . The impurity phases were found to be barium metal (**3**− **6**), barium oxide (**2**− **6**), and barium oxide chloride, Ba_4Cl_6O (**3** and **6**) respectively. The final refined crystallographic parameters for **2**−**6** are presented in Table 4 and selected interatomic distances and angles in Table 5. Refined anisotropic thermal displacement parameters for **2**−**6** are listed in the Supporting Information. An exemplar observed, calculated, and difference profile plot for Ba_2NCl (**2**) is shown in Figure 3 (profile plots for the other nitride halides, **3**−**6** are included in the Supporting Information).

In previous PND experiments on $Ca(Sr)_2N(X,X')$ compounds we found no ordering of halides, with the anions statistically occupying the interlayer 3*b* (0, 0, 0) site.[26−28] A similar situation is seen in these ToF PND experiments for **2**−**6**. There is sufficient contrast in the neutron scattering lengths of chlorine and bromine (9.58 and 6.80 fm respectively) that any ordering should be apparent in the diffraction data, and we find no evidence to suggest that a model in which Cl^- and Br^- are completely disordered across the 3*b* site is not the correct one. Likewise we see no evidence for disorder across the 3*b* and 3*a* sites, and so we can conclude that just as in calcium and strontium nitride chlorides and bromides, N^{3-} uniquely occupies the 3*a* site.

dx.doi.org/10.1021/ic201264u |*Inorg. Chem.* 2011, 50, 9545–9553

Table 7. Selected Interatomic Distances and Angles for $Ba_2NBr_yI_{(1-y)}$ from PXD Data at 298 K

	7	8
crystal system space group	hexagonal, $R\bar{3}m$ (No. 166)	
3 × Ba−Ba/Å	3.8011 (3)	3.8115 (1)
6 × Ba−Ba/Å	4.1489 (4)	4.1790 (2)
3 × Ba−N/Å	2.8134 (2)	2.8281 (1)
3 × Ba−X/Å	3.3990 (2)	3.4506 (1)
Ba−N−Ba/deg	95.011 (4)	95.267 (2)

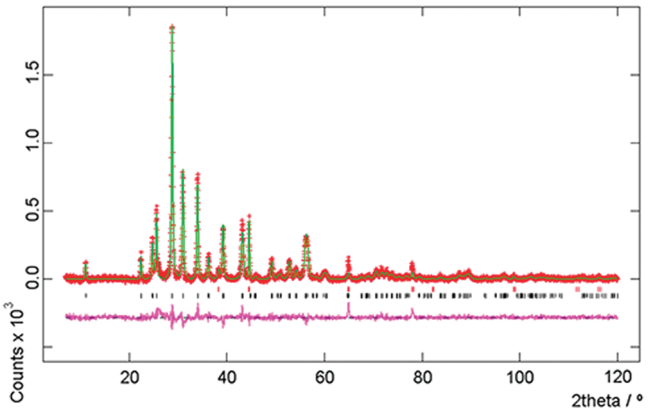

Figure 4. Rietveld refinement profile for $Ba_2NBr_{0.8}I_{0.2}$ from PXD data. Crosses indicate the observed data, the upper continuous line shows the calculated profile, and the lower continuous line the difference profile. Tick marks show reflection positions for $Ba_2NBr_{0.8}I_{0.2}$ (lower) and the aluminum sample holder (upper).

Rietveld refinements performed using PXD data collected over longer periods for **7** and **8** converged smoothly to yield good fits to the data. Peaks unaccounted for by the model could be attributed to aluminum reflections from the flat plate sample holder. The refinement results for **7** and **8** can be found in Table 6 and selected interatomic distances and angles in Table 7. The Rietveld refinement profile for **8** is shown in Figure 4. As was observed from indexing the initial X-ray data, lattice parameters increased universally with increasing bromide content as would be expected as one replaces anions with those of a larger effective ionic radius. The increase is more marked in the *c* parameter, with an increase across the series **2**−**7** of 3%, compared to a 1.2% increase in *a*. This is not unexpected, as the anions are inserted between the $[Ba_2N]^+$ layers, and one would expect anisotropic expansion. Indeed a similar pattern of increased relative expansion of *c* compared with *a* is observed in the analogous $Ca_2NCl_{(1-y)}Br_y$ and $Sr_2NCl_{(1-y)}Br_y$ ($0 \le y \le 1$) series.[26,27] With the introduction of iodide, the increasing size of the halide anion again results in larger lattice parameters, with a slightly more marked relative increase in *c* than *a*. Between **7** and **8** there is a 0.45% increase in *c* compared with a 0.1% increase in *a*.

Considering the important interatomic distances and angles for **2**−**8** (Tables 5 and 7), the configuration of the Ba−N layers in the materials does not change greatly on going across the series. The Ba−Ba distances in the *ab* plane increase from 4.1023(1) to 4.1790(1) Å from **2**−**8** (cf. 4.0290 Å in Ba_2N). In the *c* direction, within the layer, the Ba−Ba distance changes from 3.7796(1) to 3.8115(1) Å from **2**−**8** (3.7952 Å in Ba_2N).

Table 8. Layer Thickness (t), Interlayer Distances (d), Mean X Anionic Radius (X_{av}), and Mean X Pauling Electronegativity (χ_P) for $Ba_2N(X,X')$ Nitride Halides (1−8)

compound	c/a	t/Å	d/Å	t/d	X_{av} radius/Å	χ_P (X_{av})
Ba_2NF (**1**)	4.961	3.142	3.518	0.89	1.19	3.98
Ba_2NCl (**2**)	5.526	2.951	4.604	0.64	1.67	3.16
$Ba_2NCl_{0.8}Br_{0.2}$ (**3**)	5.524	2.945	4.641	0.63	1.70	3.12
$Ba_2NCl_{0.6}Br_{0.4}$ (**4**)	5.571	2.932	4.722	0.62	1.73	3.08
$Ba_2NCl_{0.4}Br_{0.6}$ (**5**)	5.603	2.931	4.793	0.61	1.76	3.04
$Ba_2NCl_{0.2}Br_{0.8}$ (**6**)	5.631	2.929	4.840	0.61	1.79	3
Ba_2NBr (**7**)	5.621	2.939	4.831	0.61	1.82	2.96
$Ba_2NBr_{0.8}I_{0.2}$ (**8**)	5.661	2.935	4.912	0.60	1.87	2.9

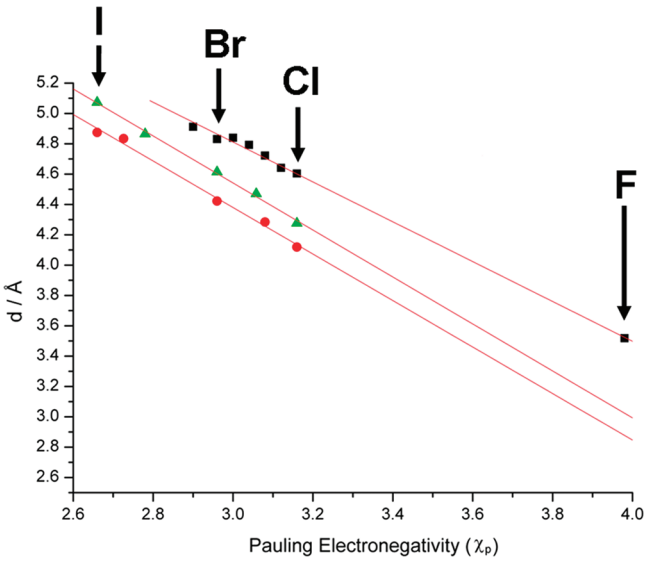

Figure 5. Plot of average X site Pauling electronegativity (χ_p) against interlayer separation (d). Squares represent the $Ba_2N(XX')$ series (**1**−**8**). Triangles represent a series of $Sr_2N(XX')$ values obtained from ref 27. Circles show a series of $Ca_2N(XX')$ values from ref 26. Lines show best linear fits to the data series.

Equally the changes in Ba−N bond lengths are quite small across the whole series, from 2.8790(1) in **2** through to 2.8281(1) Å in **8**. The corresponding length in the unfilled nitride is 2.7675 Å. More substantial changes occur in the Ba−X distances as might be expected on intercalating larger halide ions between the layers. The Ba−Cl distance in **2** is 3.2981(1) Å. The binary chloride $BaCl_2$ has two chlorine sites and a total of nine Ba−Cl distances.[46] Seven of these are shorter (2.86(8)−3.25(8) Å), with two longer out of plane distances (3.58(8) Å). Therefore, the bond distance in our layered material lies between these shorter and longer values from the binary chloride. $BaBr_2$ and BaI_2 are isostructural with the chloride, and a similar pattern is seen with the Ba−X distance in the layered nitride halide having a value between the shorter and longer Ba−X value in the corresponding binary material.

An alternative perspective when assessing the evolution in structure with X (and A) in these systems is to consider the variations in layer thickness (t) and interlayer distance (d). These are summarized in Table 8 for all the compounds, **1**−**8**. In general, increasing the size of the intercalated halide decreases t

dx.doi.org/10.1021/ic201264u |*Inorg. Chem.* 2011, 50, 9545–9553

	F	Cl	Br	I
Mg	Mg_2NF			
	$Mg_2NF^{\dagger}$	X	X	X
	Mg_3NF_3			
Ca	Ca_2NF			
	Ca_2NF	Ca_2NCl	Ca_2NBr	Ca_2NI
	Ca_2NF			
Sr	Sr_2NF	Sr_2NCl	Sr_2NBr	Sr_2NI
	Sr_2NF			
Ba	Ba_2NF	Ba_2NCl	Ba_2NBr	Ba_6NI_9
	Ba_2NF			

Tetragonal *I4$_1$/amd*	Cubic; anion disordered *Fm-3m*	Cubic; anion ordered *Fd-3m*	Hexagonal *R-3m*
Cubic; anion ordered *Pm3m*	Structure Unknown	Hexagonal *P6$_3$/mmc*	X: Compound(s) not known

Figure 6. Schematic overview of ternary A−N−X (A = Mg−Ba; X = F−I) compounds by composition and structure type.

while increasing d. Remarkable is the value of the t/d ratio for Ba_2NF compared with other nitride halides. In the former case, the values of t and d are quite similar reflecting the near parity in anionic radius between N^{3-} and F^-.[44] At these values of t/d (c/a), one would thus assume, it becomes favorable for anionic disorder and transition from the α-$NaFeO_2$ structure to a simple rock salt structure. The observation that all the compounds containing heavier halides, **2**−**8**, crystallize in the $R\bar{3}m$ space group is perhaps not unexpected since all have a t/d ratio less than the nitride fluorides but above 0.5, which correlates to the minimum value for the stability of the *anti*-α-$NaFeO_2$ structure.[26] For $t/d < 0.5$, the layered materials adopt the *anti*-β-$RbScO_2$ structure (e.g., Ca_2NI), with an HCP rather than CCP arrangement of the layers.

One can also consider the value of d with respect to the Pauling electronegativity (χ_p) of the halide X (X′). The average electronegativity of the site can be calculated for $Ba_2N(X,X')$ as

$$\chi_{paverage} = (\chi_p(X)(1-y)) + (\chi_p(X')y) \quad (3)$$

The relationship of χ_p against d is represented for **1**−**8** in Figure 5, together with related strontium and calcium materials. There is a linear relationship between the electronegativity and the layer separation with a series of almost parallel lines displaced to lower d as one ascends group 2. It is possible through extrapolation of the linear fits to estimate values for the interlayer spacings for hexagonal Sr_2NF (~3.03 Å) and Ca_2NF (~2.88 Å). These distances are significantly smaller than those in any of the hexagonal α-$NaFeO_2$ structured nitride halides (and those in the A_2N parent binary subnitrides) and this (i.e., minimization of $[A_2N]^+$ layer repulsion) is probably one of the driving forces behind the favorability of the three-dimensional, simple, and superstructured rock salt phases adopted by strontium and calcium nitride fluorides versus the observation of both layered and simple rock salt structures for Ba_2NF (Figure 6).

CONCLUSIONS

A series of new barium nitride halide layered materials have been synthesized and characterized. In the case of the fluoride material Ba_2NF, this represents the first example of an alkaline earth metal nitride fluoride crystallizing with a hexagonal layered structure. This phase appears to form in competition with the previously reported cubic rock salt phase of Ba_2NF (which is present in this study as a minor component). Further understanding of the phase relationship in this and other A_2NF materials might be forthcoming using variable temperature diffraction.

Compounds containing the heavier halides form hexagonal α-$NaFeO_2$-type structures by analogy to the equivalent calcium and strontium compounds. A complete series of quaternary nitride halides is formed between the end members Ba_2NCl and Ba_2NBr with the c parameter increasing as the Br^- anion replaces Cl^-.

The solubility of I^- in this structure type reaches a limit close to the composition $Ba_2NBr_{0.8}I_{0.2}$. Attempts to synthesize materials containing higher proportions of I^- led to the growth of an additional phase that we are currently investigating. It is possible that the new phase is related to the Ba_6NI_9 composition proposed by Ehrlich et al. from melting point analysis of mixtures of "Ba_3N_2" and BaI_2, although there is no direct match of the reflections we observe to the earlier diffraction patterns. All of the investigated nitride halides exhibit weak, temperature-independent magnetism.

ASSOCIATED CONTENT

Supporting Information. PXD analysis of Ba_2N starting material, tables of anisotropic temperature factors from powder neutron diffraction refinements for (**1**−**6**), and additional profile plots from the refinements. This material is available free of charge via the Internet at http://pubs.acs.org.

AUTHOR INFORMATION

Corresponding Author

*E-mail: duncan.gregory@glasgow.ac.uk.

Present Addresses

⊥AWE, Aldermaston, Reading, Berkshire RG7 4PR, United Kingdom.

ACKNOWLEDGMENT

We thank the ILL, France and ISIS, RAL, U.K., for the provision of beamtime associated with this work. D.H.G. and P.H. thank ENEA C.R., Brasimone, for funding a studentship for A.S.B. D.H.G. thanks WestCHEM for funding R.W.H. as a WestCHEM fellow.

REFERENCES

(1) DiSalvo, F. J. *Science* **1990**, *247*, 649.
(2) DiSalvo, F. J.; Clarke, S. J. *Curr. Opin. Solid State Mater. Sci.* **1996**, *1*, 241.
(3) Gregory, D. H. *J. Chem. Soc., Dalton Trans.* **1999**, 259.
(4) Simon, A. *Coord. Chem. Rev.* **1997**, *163*, 253.
(5) Gregory, D. H. *Coord. Chem. Rev.* **2001**, *215*, 301.
(6) von Stackelberg, M.; Paulus, R. *Z. Phys. Chem.* **1933**, *B22*, 305.
(7) Partin, D. E.; Williams, D. J.; O'Keefe, M. *J. Solid State Chem.* **1997**, *132*, 56.
(8) Gregory, D. H.; Barker, M. G.; Edwards, P. P.; Siddons, D. J. *Inorg. Chem.* **1995**, *34*, 5195.
(9) Gregory, D. H.; Bowman, A.; Baker, C. F.; Weston, D. P. *J. Mater. Chem.* **2000**, *10*, 1635.
(10) Brese, N. E.; O'Keeffe, M. *J. Solid State Chem.* **1990**, *87*, 134.
(11) Reckeweg, O.; DiSalvo, F. J. *Solid State Sci.* **2002**, *4*, 575.
(12) Ehrlich, P.; Deissmann, W. *Angew. Chem.* **1958**, *70*, 656.

(13) Ehrlich, P.; Deissmann, W.; Koch, E.; Ullrich, V. *Z. Anorg. Allg. Chem.* **1964**, *328*, 243.
(14) Emons, H.-H.; Anders, D.; Roewer, R.; Vogt, F. *Z. Anorg. Allg. Chem.* **1964**, *333*, 99.
(15) Emons, H.-H.; Grothe, W.; Seyfarth, H.-H. *Z. Anorg. Allg. Chem.* **1968**, *363*, 191.
(16) Andersson, S. *J. Solid State Chem.* **1970**, *1*, 306.
(17) Ehrlich, P.; Linz, W.; Seifert, H. J. *Naturwissenschaften* **1971**, *4*, 219.
(18) Hadenfeldt, C.; Herdejürgen, H. *Z. Anorg, Allg. Chem.* **1987**, *545*, 177.
(19) Hadenfeldt, C.; Herdejürgen, H. *Z. Anorg, Allg. Chem.* **1988**, *558*, 35.
(20) Nicklow, R. A.; Wagner, T. R.; Raymond, C. C. *J. Solid State Chem.* **2001**, *160*, 134.
(21) Wagner, T. R. *J. Solid State Chem.* **2002**, *169*, 13.
(22) Seibel, H.; Wagner, T. R. *J. Solid State Chem.* **2004**, *177*, 2772.
(23) Jack, D. R.; Zeller, M.; Wagner, T. R. *Acta Crystallogr.* **2005**, *C61*, i6.
(24) Fang, C. M.; Ramanujachary, K. V.; Hintzen, H. T.; de With, G. *J. Alloys Compds.* **2003**, *351*, 72.
(25) Bowman, A.; Mason, P. V.; Gregory, D. H. *Chem. Commun.* **2001**, *351*, 1650.
(26) Bowman, A.; Smith, R. I.; Gregory, D. H. *J. Solid State Chem.* **2005**, *178*, 1807.
(27) Bowman, A.; Smith, R. I.; Gregory, D. H. *J. Solid State Chem.* **2006**, *179*, 130.
(28) Brogan, M. A.; Hughes, R. W.; Smith, R. I.; Gregory, D. H. *Dalton Trans.* **2010**, *39*, 7153.
(29) Barker, M. G.; Begley, M. J.; Edwards, P. P.; Gregory, D. H.; Smith, S. E. *J. Chem. Soc., Dalton Trans.* **1996**, 1.
(30) Boultif, A.; Louer, D. *J. Appl. Crystallogr.* **1991**, *24*, 987.
(31) Larson, A. C.; von Dreele, R. B. *The General Structure Analysis System*; Los Alamos National Laboratories: Los Alamos, NM, 2000.
(32) Toby, B. H. *J. Appl. Crystallogr.* **2001**, *34*, 210.
(33) Reckeweg, O.; DiSalvo, F. J. *Z. Kristallogr. NCS* **2005**, *220*, 519.
(34) Künzel, H.-T. Doctoral Thesis, Universität Stuttgart, Stuttgart, Germany, 1980.
(35) Seeger, O. Doctoral Thesis, Universität Stuttgart, Stuttgart, Germany, 1994.
(36) Steinbrenner, U. Doctoral Thesis, Universität Stuttgart, Stuttgart, Germany 1997.
(37) Schultz-Coulon, V. Doctoral Thesis, Universität Bayreuth, Bayreuth, Germany 1998.
(38) Vajenine, G. V.; Grzechnik, A.; Syassen, K.; Loa, I.; Hanfland, M.; Simon, A. *C. R. Chim.* **2005**, *8*, 1897.
(39) Sears, V. F. *Neutron News* **1992**, *3* (3), 26.
(40) Wegner, B.; Essman, R.; Bock, J.; Jacobs, H. *Eur. J. Solid State Inorg. Chem.* **1992**, *29*, 1217.
(41) Gerlach, W. *Z. Phys.* **1922**, *9*, 184–192.
(42) Radtke, A.; Brown, G. *Am. Mineral.* **1974**, *59*, 885–888.
(43) Leger, J.; Haines, J.; Atouf, A.; Schulte, O.; Hull, S. *Phys. Rev. B* **1995**, *52*, 13247.
(44) Campos, A.; Quintana, P.; West, A. *J. Solid State Chem.* **1990**, *86*, 129–130.
(45) Shannon, R. D. *Acta Crystallogr.* **1976**, *A32*, 751.
(46) Brackett, E.; Brackett, T.; Sass, R. *J. Phys. Chem.* **1963**, *67*, 2132–2135.